Nonlinear interrogation of quantum materials: why higher order response tells you more

Peter P. Orth (Saarland University)

Physics Colloquium, Missouri S&T, April 13, 2023

Quantum materials: what are they?

- Materials whose often exotic properties are governed by quantum mechanics
  - Quantum properties of electronic wavefunction matter: topology & geometry
  - Coulomb interactions between electrons results in entangled wavefunction (beyond Fermi statistics)
- Prominent examples of recent interest
  - (Magnetic) Topological insulators and semimetals
  - Quantum spin liquids and spin ices
  - Unconventional superconductors
  - Quantum critical materials

Hasan, Kane (2010); Armitage, Mele, Vishwanath (2018); Keimer, Moore (2017); Savary, Balents (2017); Sigrist, Ueda (1991); Sachdev (1999); Sachdev (2023)

Quantum (spin) Hall insulators

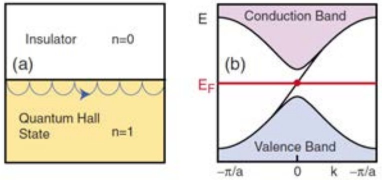

Weyl semimetal

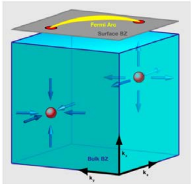

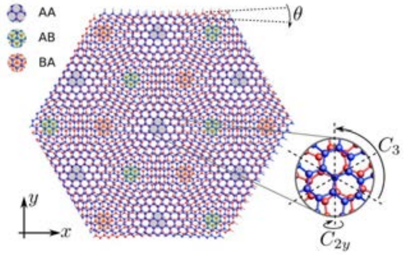

Twisted bilayer graphene

Bilayer device with magnetic TI $MnBi_2Te_4$

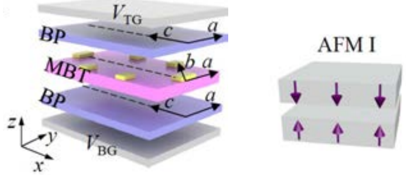

Electronic wavefunctions in solids

- Electrons in solids often well described by Bloch Hamiltonian

$$H = \frac{p^2}{2m} + V(\boldsymbol{r}) \text{ with periodic potential } V(\boldsymbol{r} + \boldsymbol{R}_\ell) = V(\boldsymbol{r})$$

- Hamiltonian commutes with unitary translation operators $T_{\boldsymbol{R}_\ell} |\psi_{n\boldsymbol{k}}\rangle = e^{i\boldsymbol{k}\cdot\boldsymbol{R}_\ell} |\psi_{n\boldsymbol{k}}\rangle$

- Momentum eigenstates $\psi_{nk}(\boldsymbol{r}) = e^{i\boldsymbol{k}\cdot\boldsymbol{r}} u_{n\boldsymbol{k}}(\boldsymbol{r})$
  - cell-periodic Bloch wavefunction $u_{nk}(r)$

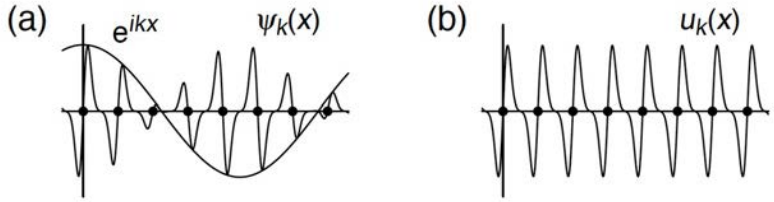

Energy dispersion E_{nk}

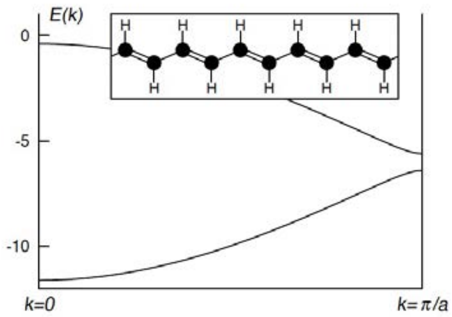

Vanderbilt (2018)

Topological Berry phase and Berry curvature

UNIVERSITÄT DES SAARLANDES

- Berry phase of a spin in a magnetic field $H = -\gamma \mathbf{B} \cdot \mathbf{S} = -\left(\frac{\gamma \hbar B}{2}\right) \hat{\mathbf{n}} \cdot \boldsymbol{\sigma}$

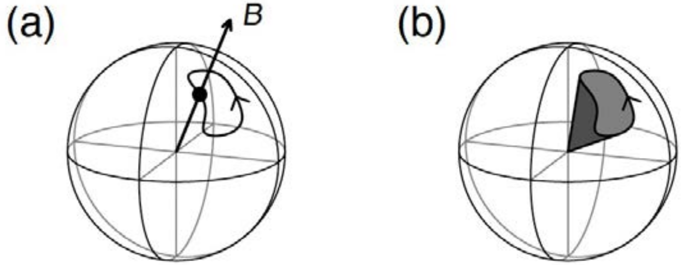

Up-spin eigenfunction

$$|\uparrow_{\hat{\mathbf{n}}}\rangle = \begin{pmatrix} \cos(\theta/2) \\ \sin(\theta/2) e^{i\varphi} \end{pmatrix}$$

- Berry phase is geometric phase picked up during transport along closed loop

$$\phi = \oint \langle u_\lambda | i \partial_\lambda u_\lambda \rangle \, d\lambda \, . \quad \Rightarrow \quad \phi = \oint_P \mathbf{A} \cdot d\boldsymbol{\lambda} = \int_S \boldsymbol{\Omega} \cdot \hat{\mathbf{n}} \, dS = \int_S \boldsymbol{\Omega} \cdot d\mathbf{S}$$

Berry connection (gauge potential)

Berry curvature or flux (gauge invariant)

$$\Omega_{\mu\nu} = \partial_\mu A_\nu - \partial_\nu A_\mu = -2 \, \mathrm{Im} \, \langle \partial_\mu u | \partial_\nu u \rangle \, .$$

Vanderbilt (2018)

Topological Berry phase and Berry curvature

- Berry phase of a spin in a magnetic field $H = -\gamma \mathbf{B} \cdot \mathbf{S} = -\left(\frac{\gamma \hbar B}{2}\right) \hat{\mathbf{n}} \cdot \boldsymbol{\sigma}$

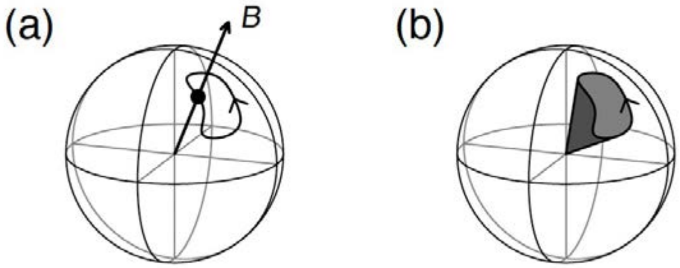

Up-spin eigenfunction

$$|\uparrow_{\hat{\mathbf{n}}}\rangle = \begin{pmatrix} \cos(\theta/2) \\ \sin(\theta/2) e^{i\varphi} \end{pmatrix}$$

Close to north pole

$$|\uparrow_{\hat{\mathbf{n}}}\rangle \simeq \begin{pmatrix} 1 \\ (n_x + i n_y)/2 \end{pmatrix}$$

$$|\partial_{n_x} \uparrow_{\hat{\mathbf{n}}}\rangle = \frac{1}{2}\begin{pmatrix} 0 \\ 1 \end{pmatrix}, \quad |\partial_{n_y} \uparrow_{\hat{\mathbf{n}}}\rangle = \frac{1}{2}\begin{pmatrix} 0 \\ i \end{pmatrix}.$$

- Berry phase = flux through shaded area $\phi = \int_S \boldsymbol{\Omega} \cdot d\mathbf{S}$

Constant Berry flux $\Omega_z = -1/2$

Berry phase is proportional to shaded area

$$\Omega_{\mu\nu} = \partial_\mu A_\nu - \partial_\nu A_\mu = -2\,\mathrm{Im}\,\langle \partial_\mu u | \partial_\nu u \rangle . \quad \Omega_\kappa = \frac{1}{2} \epsilon_{\mu\nu\kappa} \Omega_{\mu\nu}$$

Vanderbilt (2018)

Berry phase of Bloch electrons in solids

- Bloch Hamiltonian $H_{ij}(k)$ resembles spin in magnetic field $\hat{H} = \sum_{ij} \sum_{\mathbf{k}} H_{ij}(\mathbf{k}) \hat{a}^{\dagger}_{i\mathbf{k}} \hat{a}_{j\mathbf{k}}.$
- Example: Weyl semimetal $H_{\pm} = \pm v \sum_{i=x,y,z} k_i \sigma_i$

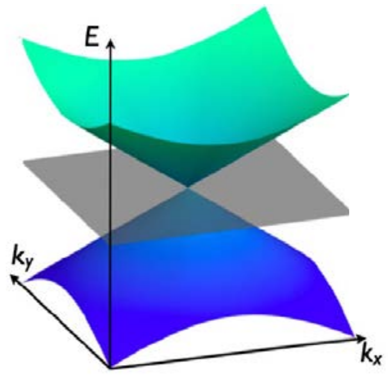

$k_z = 0$

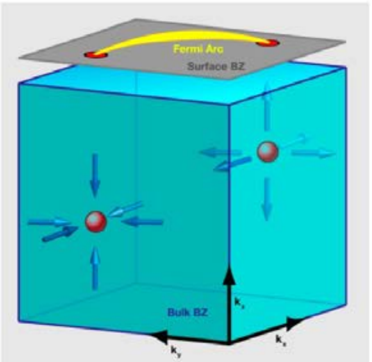

Armitage *et al.* (2018)

- Berry connection $A_n(k) = \langle u_{nk} | i \nabla_k | u_{nk} \rangle$
- Berry phase $\phi_n = \oint_C dk \cdot A_n(k)$
- Berry curvature $\Omega_n(k) = \nabla_k \times A_n(k)$
- Weyl points are sources of Berry flux (magnetic monopoles) $\oint \mathbf{\Omega} \cdot \mathbf{dS} = \mp 2\pi$

Impact of Berry curvature on electronic transport

- Berry curvature acts like a magnetic field in momentum space
- Semiclassical equations of motion of Bloch electrons

$$\dot{\boldsymbol{r}} = \frac{1}{\hbar}\nabla_{\boldsymbol{k}}\epsilon_{\boldsymbol{k}} - \dot{\boldsymbol{k}} \times \boldsymbol{\Omega},$$

$$\hbar\dot{\boldsymbol{k}} = -e\boldsymbol{E} - e\dot{\boldsymbol{r}} \times \boldsymbol{B}.$$

Transverse Hall current

$$K_y = \frac{-e}{(2\pi)^2}\int_{\mathrm{BZ}} f(\mathbf{k})\,\dot{y}(\mathbf{k})\,d^2k = \frac{-e}{(2\pi)^2}\int_{\mathrm{BZ}} f(\mathbf{k})\,\dot{k}_x\,\Omega(\mathbf{k})\,d^2k = \frac{-e}{(2\pi)^2}\left(\frac{-e}{\hbar}\mathcal{E}_x\right)\int_{\mathrm{BZ}} f(\mathbf{k})\,\Omega(\mathbf{k})\,d^2k$$

- Anomalous Hall conductivity

$$\sigma_{yx} = \frac{e^2}{(2\pi)^2\hbar}\int_{\mathrm{BZ}} f(\mathbf{k})\,\Omega(\mathbf{k})\,d^2k$$

Time-reversal ($\mathcal{T}$)	$\tilde{\Omega}^{(n)}_{\mu\nu}(\mathbf{k}) = -\Omega^{(n)}_{\mu\nu}(-\mathbf{k})$
Inversion (P)	$\tilde{\Omega}^{(n)}_{\mu\nu}(\mathbf{k}) = \Omega^{(n)}_{\mu\nu}(-\mathbf{k})$
$P\mathcal{T}$	$\tilde{\Omega}^{(n)}_{\mu\nu}(\mathbf{k}) = -\Omega^{(n)}_{\mu\nu}(\mathbf{k})$

Nonzero only in absence of time-reversal symmetry

How to probe Berry curvature in presence of TR?

Types of nonlinear probes of quantum materials

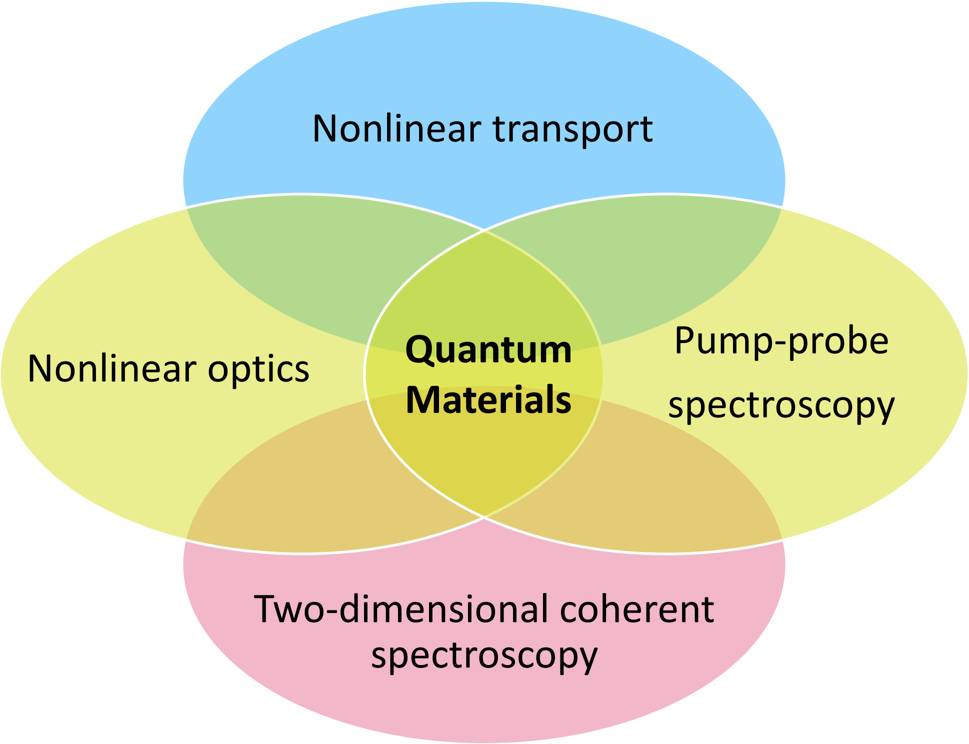

Basic concepts of nonlinear probes 1

- Nonlinear response described by higher-rank tensors

$$P_i = \sum_j \chi^{(1)}_{ij} E_j + \sum_{j,k} \chi^{(2)}_{ijk} E_j E_k + \sum_{j,k,l} \chi^{(3)}_{ijkl} E_j E_k E_l + \ldots$$

- Obey different symmetry constraints than linear response

- Detect symmetries & symmetry breaking (example: second-harmonic generation)

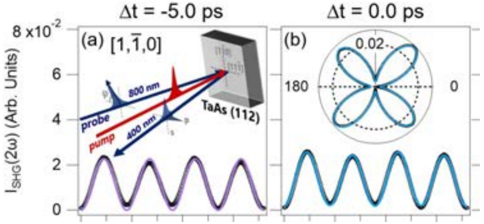

From Sirica, PPO *et al.* (2022)

Fiebig *et al.* (2005);
Zhao, Torchinsky, Hsieh *et al.* (2018)

Basic concepts of nonlinear probes 2

- Nonlinear response probes topology and quantum geometry

$$\boxed{\mathcal{Q}^{(n)}_{\mu\nu}(\mathbf{k}) = \langle \partial_\mu u_n | \partial_\nu u_n \rangle - \langle \partial_\mu u_n | u_n \rangle \langle u_n | \partial_\nu u_n \rangle}$$
$$= g^{(n)}_{\mu\nu}(\mathbf{k}) - \frac{i}{2}\Omega^{(n)}_{\mu\nu}(\mathbf{k}) \;,$$

Time-reversal ($\mathcal{T}$)	$\tilde{\Omega}^{(n)}_{\mu\nu}(\mathbf{k}) = -\Omega^{(n)}_{\mu\nu}(-\mathbf{k})$
Inversion (P)	$\tilde{\Omega}^{(n)}_{\mu\nu}(\mathbf{k}) = \Omega^{(n)}_{\mu\nu}(-\mathbf{k})$
$P\mathcal{T}$	$\tilde{\Omega}^{(n)}_{\mu\nu}(\mathbf{k}) = -\Omega^{(n)}_{\mu\nu}(\mathbf{k})$

- Example: Nonlinear Hall effect due to Berry curvature dipole

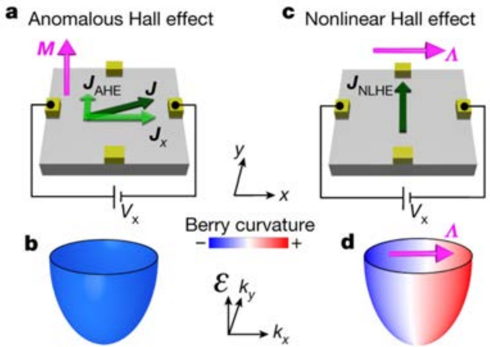

$$\sigma_{yx} = \frac{e^2}{(2\pi)^2\hbar}\int_{\mathrm{BZ}} f(\mathbf{k})\,\Omega(\mathbf{k})\,d^2k\;,$$

$$\chi_{abc} = \varepsilon_{adc}\frac{e^3\tau}{2(1+i\omega\tau)}\int_k (\partial_b f_0)\Omega_d.$$

From Ma *et al.* (2018):

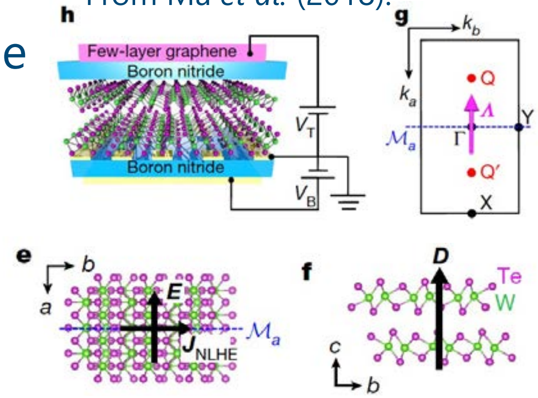

Sodemann, Fu (2014; Ma *et al.* (2018); Kang *et al.* (2018)

Basic concepts of nonlinear probes 3

- Nonlinear response can be viewed as lower-order response in perturbed system
- Perturbative example: circular photogalvanic effect (CPGE) due to BC dipole
- Multiple weak-pulses: 2D spectroscopy (discussed later)
- Pump-probe is highly nonlinear example of probing excited states.

$$\mathbf{j} = e \int \frac{d^2k}{4\pi^2} [\dot{\mathbf{k}} \times \mathbf{\Omega}(\mathbf{k})] g(\mathbf{k}),$$

$$g(\mathbf{k}) = \left(\frac{e\mathbf{E} \cdot \mathbf{v}_n(\mathbf{k})}{1/\tau - i\omega} + \text{c.c.} \right) \left(\frac{\partial f}{\partial \epsilon} \right)_0$$

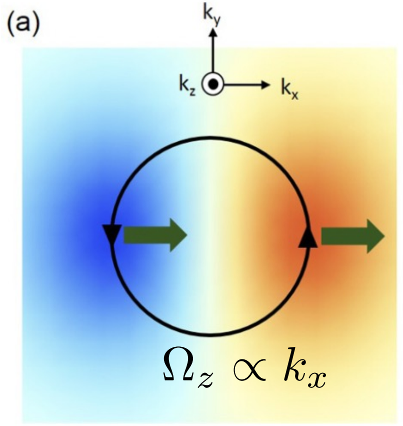

$$\dot{\boldsymbol{r}} = \frac{1}{\hbar} \nabla_{\boldsymbol{k}} \epsilon_{\boldsymbol{k}} - \dot{\boldsymbol{k}} \times \boldsymbol{\Omega},$$

$$\hbar \dot{\boldsymbol{k}} = -e\boldsymbol{E} - e\dot{\boldsymbol{r}} \times \boldsymbol{B}.$$

Moore, Orenstein (2010)
Sodemann, Fu (2014)
Chan et al. (2017, 2018)
Ma *et al.* (2017)

Why probing quantum materials nonlinearly?

Nonlinear interrogation of materials provides information about

- Electronic symmetry & hidden orders via symmetry breaking
- Topology & quantum geometry of Bloch wavefunctions
- Nature, lifetimes & couplings of excitations
- Quantum coherences of the many-body quantum state

Examples from:

- Sirica, PPO *et al.*, Nat. Mater. (2022).
- Qiang,…, PPO, arXiv:2301.11243.
- Xu,.., PPO,.., Wang, Nat. Mater (2018).

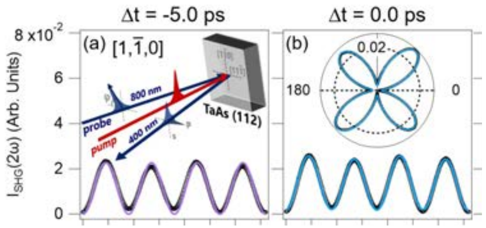

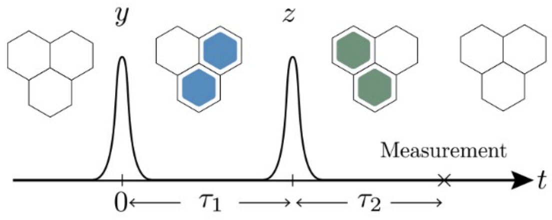

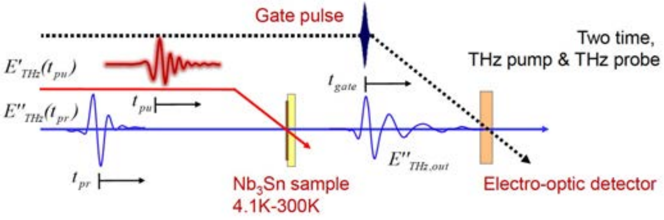

Collaborators

Theory collaborators

- Yihua Qiang, Victor Quito (Ames Lab)
- Thais V. Trevisan (UC Berkeley)
- Mathias S. Scheurer (Innsbruck Univ)

Experimental collaborators

UNIVERSITÄT DES SAARLANDES

- Nick Sirica, Rohit Prasankumar, Dmitry Yarotski (Los Alamos National Lab)
- Jigang Wang (Ames Lab)
- Qiong Ma (Boston College)
- Suyang Xu (Harvard)


N. Sirica


R. Prasankumar


D. Yarotksi

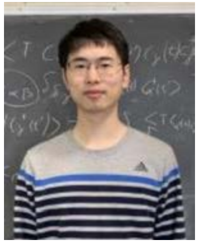
Y. Qiang


V. Quito


T. V. Trevisan


M. S. Scheurer


J. Wang

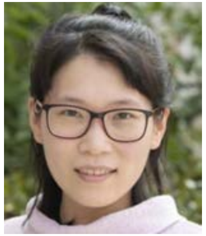
Q. Ma


S. Xu

Nonlinear optics - SHG as sensitive symmetry probe

Nonlinear response probes electronic symmetry

- Nonlinear response described by higher rank tensors
  - Example: electric polarization

$$P_i = \sum_j \chi^{(1)}_{ij} E_j + \sum_{j,k} \chi^{(2)}_{ijk} E_j E_k + \sum_{j,k,l} \chi^{(3)}_{ijkl} E_j E_k E_l + \dots$$

- Symmetry transformation imposes constraints

$$\chi_{ijk} = \sum_{i',j',k'} R_{ii'} R_{jj'} R_{kk'} \chi_{i'j'k'}$$

➢ Constraints inform us about symmetries & symmetry breaking

Second-harmonic generation (SHG)

Experimental setup

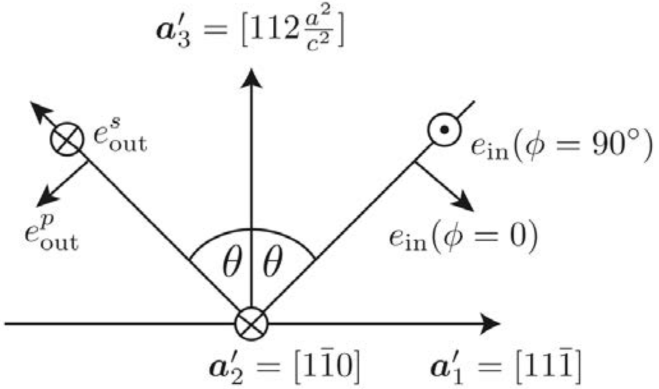

Outgoing intensities as function of incoming polarization

$$I_{\text{SHG}}^{[1\bar{1}0]}(2\omega;\phi) \propto |\boldsymbol{P}(2\omega;\phi)\cdot \boldsymbol{e}_2'|^2$$

$$I_{\text{SHG}}^{[11\bar{1}]}(2\omega;\phi) \propto |\boldsymbol{P}(2\omega;\phi)\cdot \boldsymbol{e}_1'|^2$$

$$\boldsymbol{P}_i(2\omega;\phi) = \sum_{j,k=x,y,z} \chi_{ijk}^{\text{ED}}(2\omega;\omega,\omega)\boldsymbol{E}_j(\omega;\phi)\boldsymbol{E}_k(\omega;\phi)$$

$$\chi_{ijk}^{\text{ED}} \equiv \chi_{ijk} = \left(\begin{pmatrix} xxx & xxy & xxz \\ xxy & xyy & xyz \\ xxz & xyz & xzz \end{pmatrix} \begin{pmatrix} yxx & yxy & yxz \\ yxy & yyy & yyz \\ yxz & yyz & yzz \end{pmatrix} \begin{pmatrix} zxx & zxy & zxz \\ zxy & zyy & zyz \\ zxz & zyz & zzz \end{pmatrix} \right)$$

C4v symmetry constraints

$$\chi_{ijk}^{(C_{4v})} = \left(\begin{pmatrix} 0 & 0 & xxz \\ 0 & 0 & 0 \\ xxz & 0 & 0 \end{pmatrix} \begin{pmatrix} 0 & 0 & 0 \\ 0 & 0 & xxz \\ 0 & xxz & 0 \end{pmatrix} \begin{pmatrix} zxx & 0 & 0 \\ 0 & zxx & 0 \\ 0 & 0 & zzz \end{pmatrix} \right)$$

Time-resolved SHG in Weyl semimetal TaAs

- Outgoing intensities for C_{4v} symmetry

$$I_{\mathrm{SHG}}^{[1\bar{1}0]} = a_1 \sin^2(2\phi)$$
$$I_{\mathrm{SHG}}^{[11\bar{1}]} = \left[b_1 + b_2 \cos^2(\phi)\right]^2$$

- Optical pump removes symmetries
  - ➢ Fitting of SHG allows to determine symmetry reduction

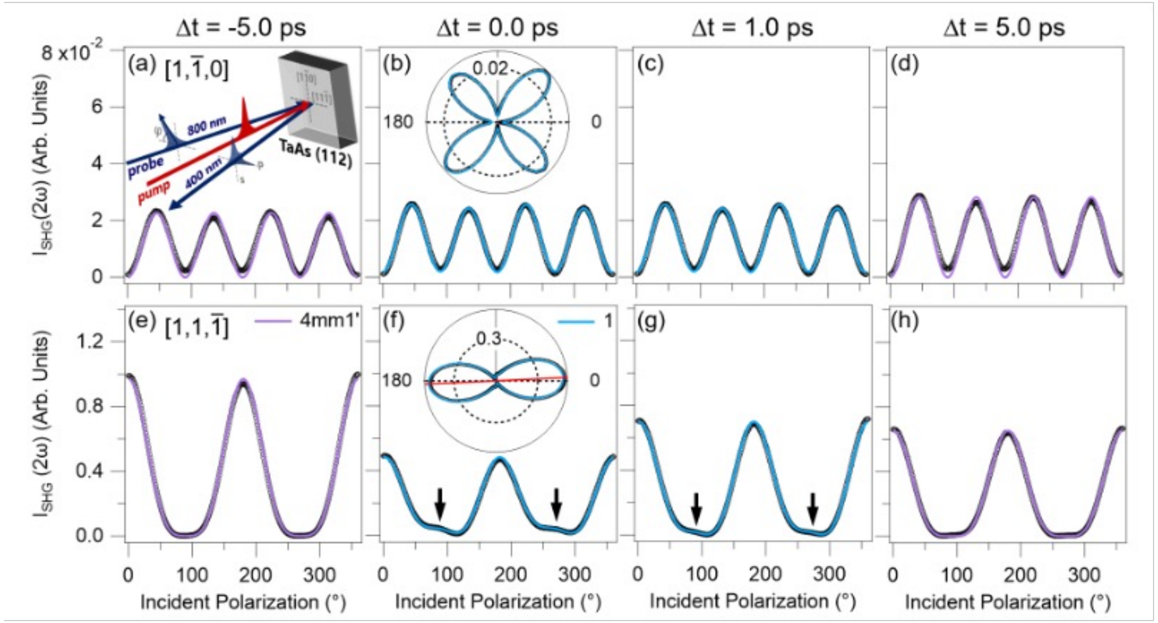

Sirica, PPO et al., Nature Materials (2022)

Microscopic origin of dynamic symmetry breaking

- All spatial symmetries and time-reversal are removed by optical pump
- Observed reduction of magnetic symmetry consistent with photocurrent generation
- Symmetry reduction can be controlled by pump polarization

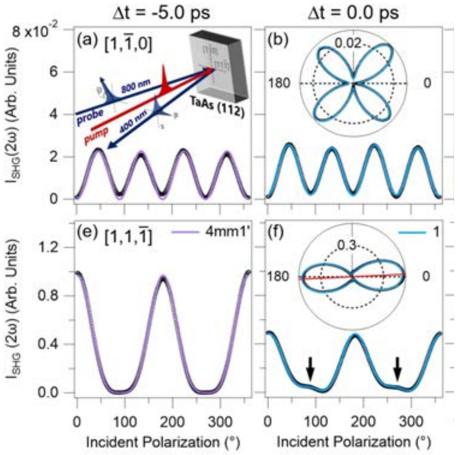

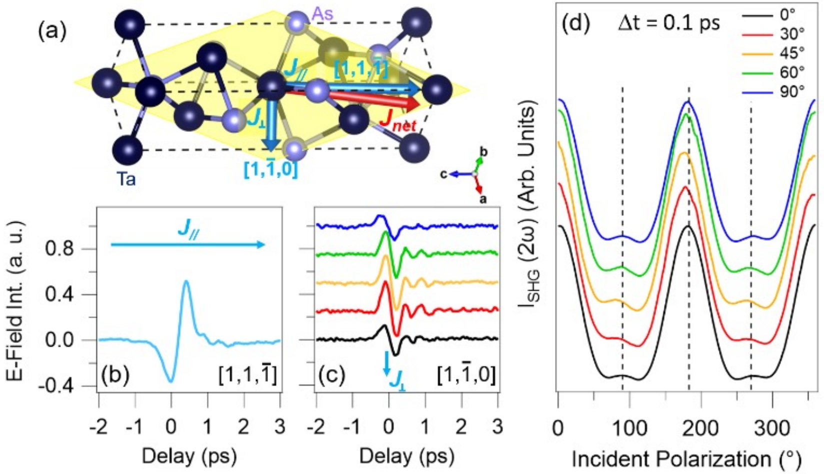

Sirica, PPO *et al.*, Nature Materials (2022).

Two-dimensional coherent spectroscopy

Two-dimensional coherent spectroscopy

- Several time-spaced light pulses irradiate the system
  - Followed by a measurement of an observable, e.g., polarization P or magnetization M
- Nonlinear susceptibility $R^{(n)}(t_1, t_2, \dots, t_n)$

Linear — Second-order

$$M_a(t) = \underbrace{\int_0^\infty ds R^{(1)}_{ab}(s) B_b(t-s)}_{\text{Linear}} + \underbrace{\int_0^\infty ds_1 \int_0^\infty ds_2 R^{(2)}_{abc}(s_1, s_2) B_b(t-s_1) B_c(t-s_2)}_{\text{Second-order}} +$$

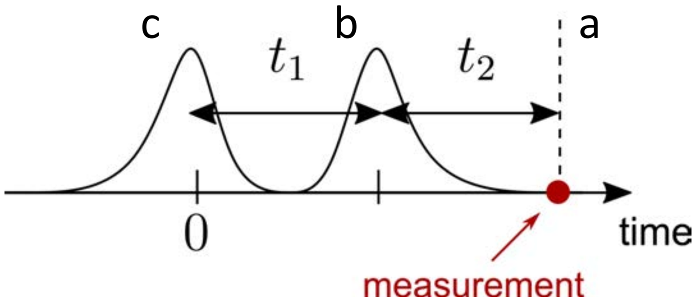

- S. Mukamel, Principles of Nonlinear Optical Spectroscopy (1999).
- P. Hamm and M. Zanni, Concepts and Methods of 2D
- Infrared Spectroscopy (2011).
- J. Lu, X. Li, Y. Zhang, H. Y. Hwang, B. K. Ofori-Okai, K. A. Nelson, Top Curr Chem (Z) **376**, 6 (2018).
- M, Woerner, W. Kuehn, P. Bowlan, K. Reimann and T. Elsaesser, New J. Phys. **15**, 025039 (2013).

Two-dimensional coherent spectroscopy

- Several time-spaced light pulses irradiate the system
  - Followed by a measurement of an observable, e.g., polarization P or magnetization M
- Nonlinear susceptibility $R^{(n)}(t_1, t_2, \ldots, t_n)$

$$M_a(t) = \underbrace{\int_0^\infty ds R^{(1)}_{ab}(s) B_b(t-s)}_{\text{Linear}} + \underbrace{\int_0^\infty ds_1 \int_0^\infty ds_2 R^{(2)}_{abc}(s_1, s_2) B_b(t-s_1) B_c(t-s_2)}_{\text{Second-order}} +$$

- Kubo formula
  - Linear response $R^{(1)}_{ab}(t_1) = \frac{i}{N}\theta(t_1)\left\langle \left[\hat{M}_a(t), \hat{M}_b(0)\right]\right\rangle_0$
  - 2nd-order response $R^{(2)}_{abc}(t_2, t_1+t_2) = \frac{i^2}{N}\theta(t_1)\theta(t_2)\left\langle \left[\left[\hat{M}_a(t_1+t_2), \hat{M}_b(t_1)\right], \hat{M}_c(0)\right]\right\rangle_0$

Correlation functions as quantum pathways

- Pathways provide useful intuition about nonlinear response
- Requires knowledge of all Hamiltonian eigenstates
  - Lehmann representation of correlation function

Ladder diagram for pathway A

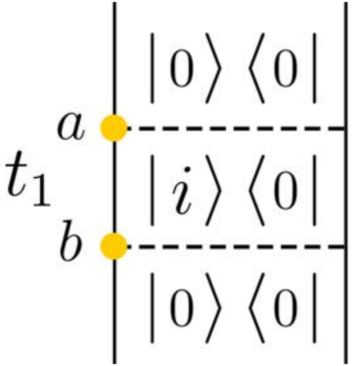

Example: Linear response

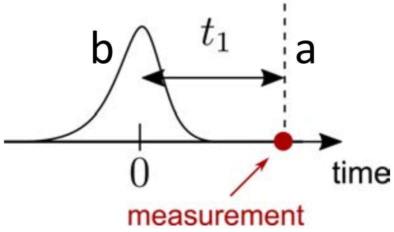

Kubo formula

$$R^{(1)}_{ab}(t_1) = \frac{i}{N}\theta(t_1)\left[\underbrace{\mathrm{tr}\left(\hat{M}_a(t_1)M_b(0)\,|0\rangle\langle 0|\right)}_{\text{Quantum pathway A}} - \underbrace{\mathrm{tr}\left(M_b(0)\hat{M}_a(t_1)\,|0\rangle\langle 0|\right)}_{\text{Quantum pathway B}}\right]$$

Quantum pathway A in linear response: step 1

$$A = \mathrm{tr}\left(e^{iHt_1}\hat{M}_a e^{-iHt_1}\hat{M}_b \left|0\right\rangle\left\langle 0\right|\right) = \mathrm{tr}\left(\hat{M}_a e^{-iHt_1}\underbrace{\hat{M}_b \left|0\right\rangle\left\langle 0\right| e^{iHt_1}}_{\text{Step 1}}\right)$$

Step 1: $\widehat{M}_b$ acts on the left of ρ_0

Created quantum coherence

$$\hat{M}_b \left|0\right\rangle\left\langle 0\right| = \sum_i \left\langle i\middle|\hat{M}_b\middle|0\right\rangle \left|i\right\rangle\left\langle 0\right| = \sum_i M_{b,i0}\left|i\right\rangle\left\langle 0\right|$$

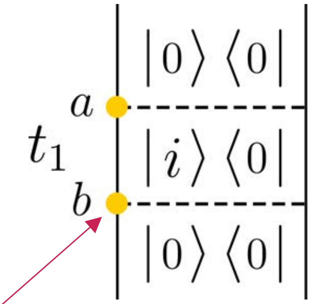

Insert resolution of identity using a basis of eigenstates of H

Transition matrix element between energy eigenstates

Quantum pathway A in linear response: step 2

$$A = \mathrm{tr}\left(e^{iHt_1}\hat{M}_a e^{-iHt_1}\hat{M}_b |0\rangle\langle 0|\right) = \mathrm{tr}\left(\hat{M}_a \underbrace{e^{-iHt_1}\underbrace{\hat{M}_b |0\rangle\langle 0|}_{\text{Step 1}} e^{iHt_1}}_{\text{Step 2}}\right)$$

Step 2: Time-evolution of the density matrix over time t_1

$$e^{-iHt_1}\hat{M}_b |0\rangle\langle 0| e^{iHt_1} = \sum_i M_{b,i0} e^{-i\omega_{i0}t_1} |i\rangle\langle 0|$$

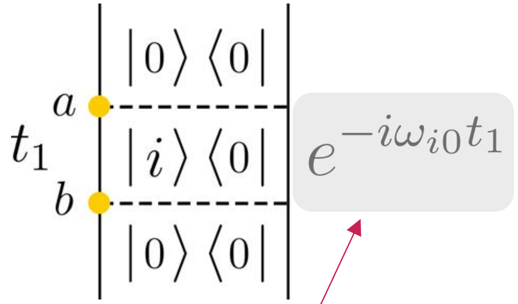

Oscillates with energy difference of states i and 0: $\omega_{i0} = E_i - E_0$

Quantum pathway A in linear response: step 3

$$A = \mathrm{tr}\left(e^{iHt_1}\hat{M}_a e^{-iHt_1}\hat{M}_b\left|0\right\rangle\left\langle 0\right|\right) = \mathrm{tr}\left(\underbrace{\hat{M}_a \underbrace{e^{-iHt_1}\underbrace{\hat{M}_b\left|0\right\rangle\left\langle 0\right|}_{\text{Step 1}} e^{iHt_1}}_{\text{Step 2}}}_{\text{Step 3}}\right)$$

Step 3: $\widehat{M}_a$ acts on the time-evolved density matrix. Perform trace → measurement

$$\mathrm{tr}\left(\hat{M}_a G(t_1)\hat{M}_b\left|0\right\rangle\left\langle 0\right|\right) = \sum_i M_{b,i0}M_{a,0i}e^{-i\omega_{i0}t_1}$$

Summation over all energy eigenstates i

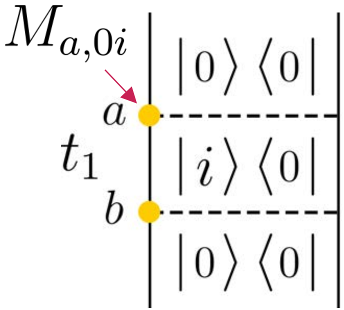

Quantum pathways A and B in linear response

$$A = \mathrm{tr}\left(e^{iHt_1}\hat{M}_a e^{-iHt_1}\hat{M}_b \left|0\right\rangle\left\langle 0\right|\right) = \mathrm{tr}\left(\hat{M}_a e^{-iHt_1}\hat{M}_b \left|0\right\rangle\left\langle 0\right| e^{iHt_1}\right)$$

$$B = \mathrm{tr}\left(\hat{M}_b e^{iHt_1}\hat{M}_a e^{-iHt_1} \left|0\right\rangle\left\langle 0\right|\right) = \mathrm{tr}\left(\hat{M}_a e^{-iHt_1} \left|0\right\rangle\left\langle 0\right| \hat{M}_b e^{iHt_1}\right)$$

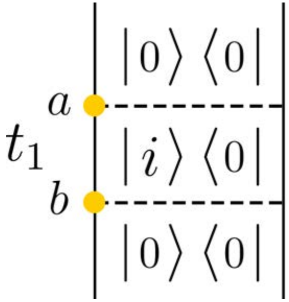

Quantum pathway A

-

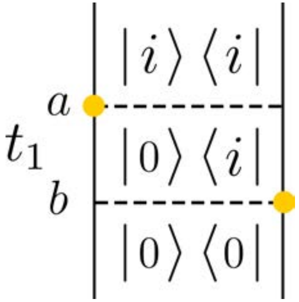

Quantum pathway B

=

Linear response

$$R^{(1)}_{ab}(t_1) = \frac{i}{N}\theta(t_1)\left[\sum_i M_{b,i0}M_{a,0i}e^{-i\omega_{i0}t_1} - \mathrm{c.c.}\right]$$

$$\xrightarrow{\text{Fourier transform}} R^{(1)}_{ab}(\omega_1)$$

Second-order response

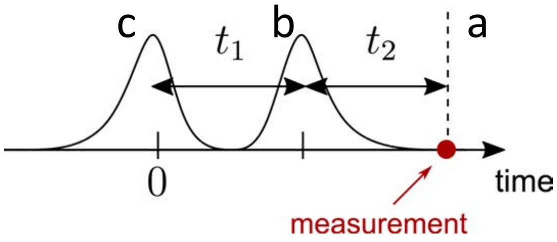

$$R^{(2)}_{abc}(t_2, t_1{+}t_2) = \frac{i^2}{N}\theta(t_1)\theta(t_2)\left\langle\left[\left[\hat{M}_a(t_1+t_2), \hat{M}_b(t_1)\right], \hat{M}_c(0)\right]\right\rangle_0 = \frac{i^2}{N}\theta(t_1)\theta(t_2)\sum_{j=1}^{2}\underbrace{\left[P^{(2)}_{j,abc}(t_1,t_2) + \mathrm{c.c}\right]}_{\text{Total of four diagrams!}}$$

$$P^{(2)}_{1,abc}(t_1,t_2) = \mathrm{tr}\left(\hat{M}_a G(t_2)\hat{M}_b G(t_1)\hat{M}_c\rho_0\right)$$

$$P^{(2)}_{2,abc}(t_1,t_2) = -\mathrm{tr}\left[\hat{M}_a G(t_2)\left(\left(G(t_1)\hat{M}_c\rho_0\right)\hat{M}_b\right)\right]$$

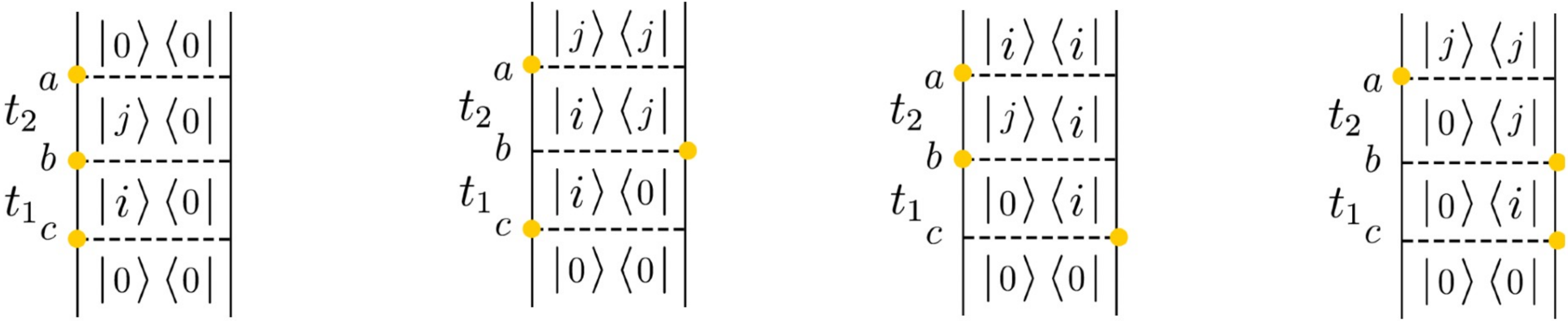

Third-order response

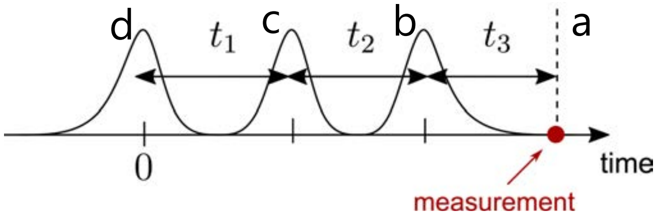

$$R^{(3)}_{abcd}(t_3, t_2+t_3, t_1+t_2+t_3) = \frac{i^3}{N}\theta(t_1)\theta(t_2)\theta(t_3)\left\langle \left[\left[\left[\hat{M}_a(t_1+t_2+t_3), \hat{M}_b(t_1+t_2)\right], \hat{M}_c(t_1)\right], \hat{M}_d(0)\right]\right\rangle_0$$

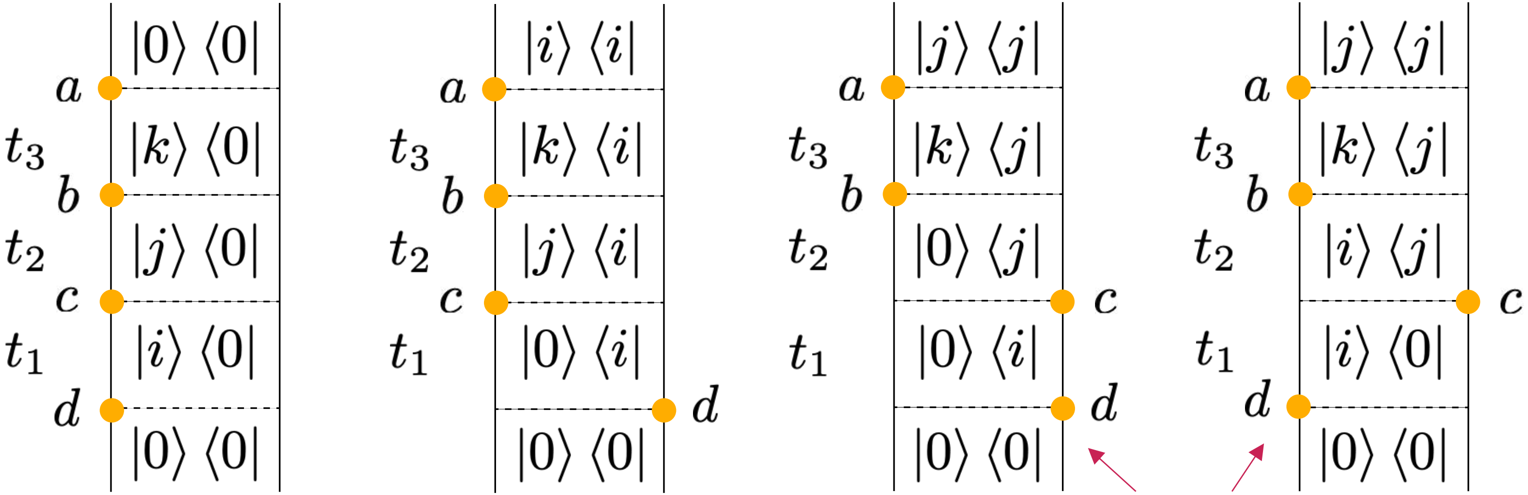

2Q-pathway Non-rephasing pathway Echo (rephasing) pathways

2D spectrum in frequency space

- Fourier transformation $\int_{-\infty}^{+\infty} dt \theta\left(t\right) e^{i\omega t - i\omega_{ij} t - \Gamma t} = g_\Gamma\left(\omega - \omega_{ij}\right)$
- The g-function contains delta function and principal value

$$g_\Gamma\left(x\right) = \frac{i}{x + i\Gamma} = iP\left(\frac{1}{x}\right) + \pi\delta\left(x\right)$$

- Terms in the 2D spectrum contain products of g functions
  - Mixing of delta function and PV contributions occur
  - Characteristic slowly decaying PV streaks coming out of localized delta function peaks in 2D spectrum

$$g_\Gamma\left(x\right) g_\Gamma(y) = \left[\pi^2\delta(x)\delta(y) - P\left(\frac{1}{x}\right) P\left(\frac{1}{y}\right)\right] + i\left[\pi\delta\left(x\right) P\left(\frac{1}{y}\right) + \pi\delta\left(y\right) P\left(\frac{1}{x}\right)\right]$$

2D coherent THz spectroscopy: Experiments

PRL 118, 207204 (2017) PHYSICAL REVIEW LETTERS week ending 19 MAY 2017

Coherent Two-Dimensional Terahertz Magnetic Resonance Spectroscopy of Collective Spin Waves

Jian Lu,[1] Xian Li,[1] Harold Y. Hwang,[1] Benjamin K. Ofori-Okai,[1] Takayuki Kurihara,[2] Tohru Suemoto,[2] and Keith A. Nelson[1,*]

[1]Department of Chemistry, Massachusetts Institute of Technology, Cambridge, Massachusetts 02139, USA

[2]Institute for Solid State Physics, The University of Tokyo, Kashiwa, Chiba 277-8581, Japan

(Received 7 October 2016; published 18 May 2017)

- Noncentrosymmetric canted AFM material $YFeO_3$.
- Two THz-active zone-center magnon modes

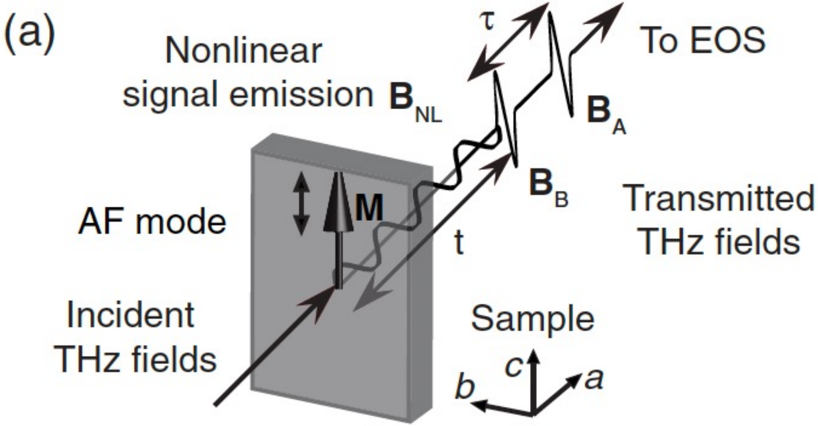

$$\mathbf{B}_{NL}(t,\tau) = \mathbf{B}_{AB}(t,\tau) - \mathbf{B}_A(t,\tau) - \mathbf{B}_B(t)$$

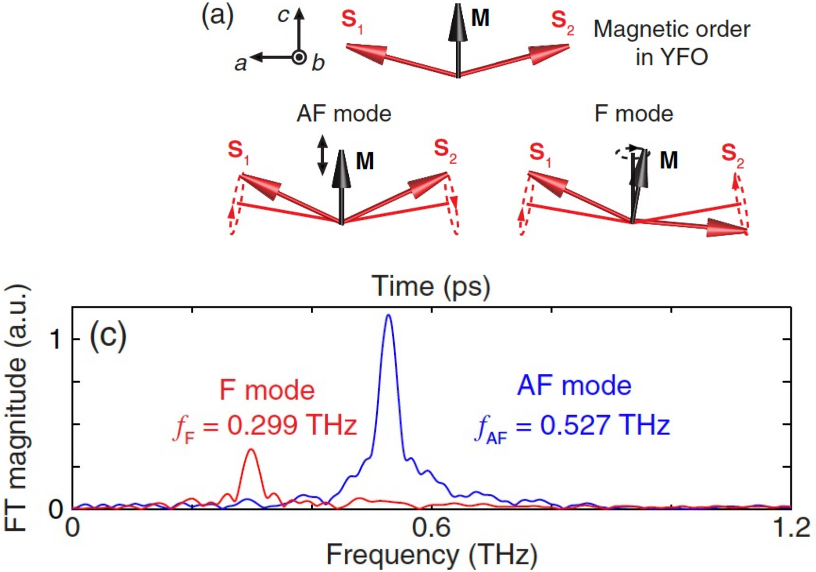

Real-time nonlinear signal for fixed pulse delay

- Different modes can be selectively excited by choice of B-field polarization

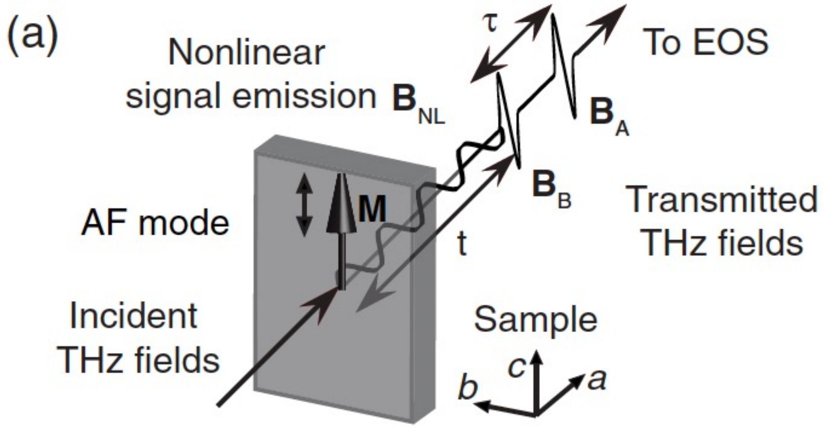

$$\mathbf{B}_{\mathrm{NL}}(t,\tau) = \mathbf{B}_{AB}(t,\tau) - \mathbf{B}_{A}(t,\tau) - \mathbf{B}_{B}(t)$$

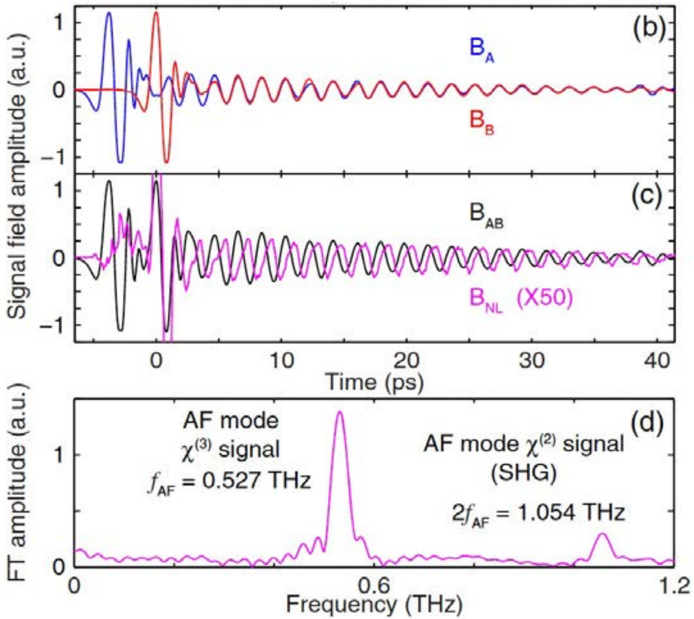

2D THz spectrum: AF mode

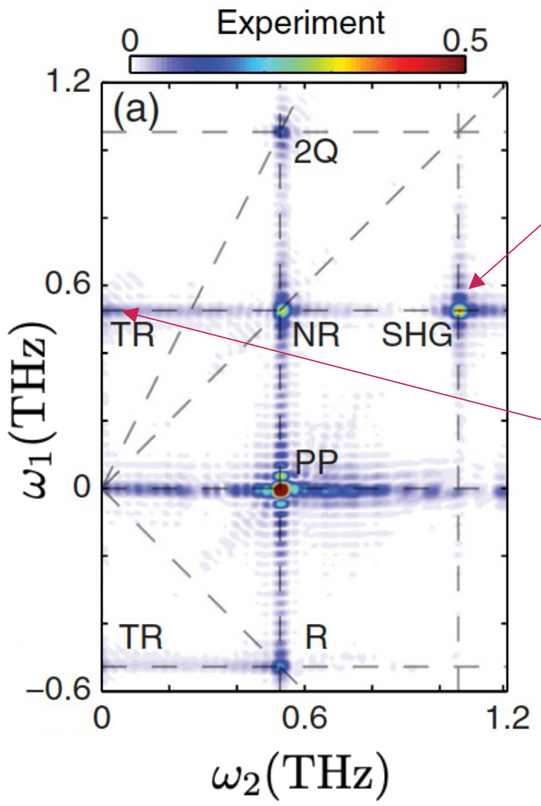

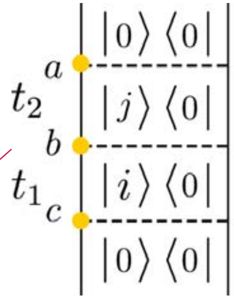

SHG pathway

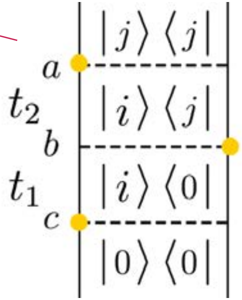

THz rectification (TR) pathway

- Both second-order signals detected
- Purely magnetic origin
- Reproduced by semiclassical LLG simulations using Hamiltonian

$$H = -J\mathbf{S}_1 \cdot \mathbf{S}_2 + \mathbf{D} \cdot (\mathbf{S}_1 \times \mathbf{S}_2) - \sum_{i=1,2} (K_a S_{ia}^2 + K_c S_{ic}^2)$$
$$- \gamma [\mathbf{B}_A^{\mathrm{THz}}(t,\tau) + \mathbf{B}_B^{\mathrm{THz}}(t)] \cdot \sum_{i=1,2} \mathbf{S}_i .$$

AF mode

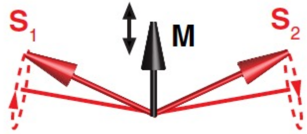

3rd order peaks in 2D THz spectrum of AF mode

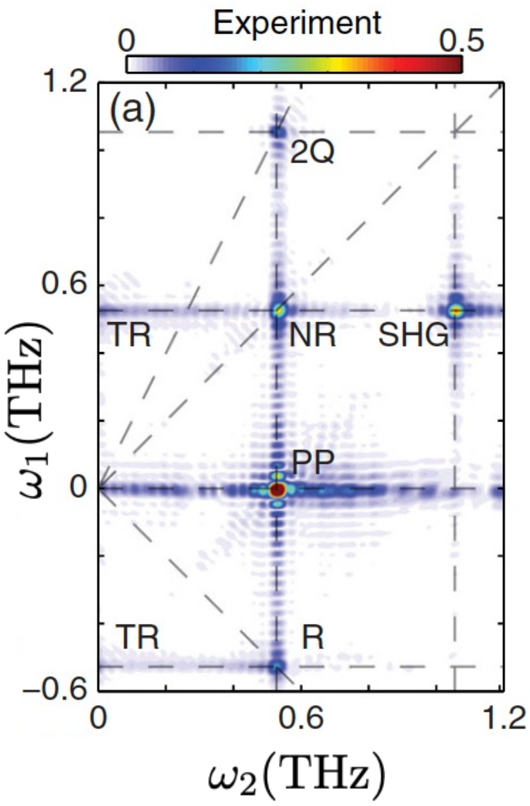

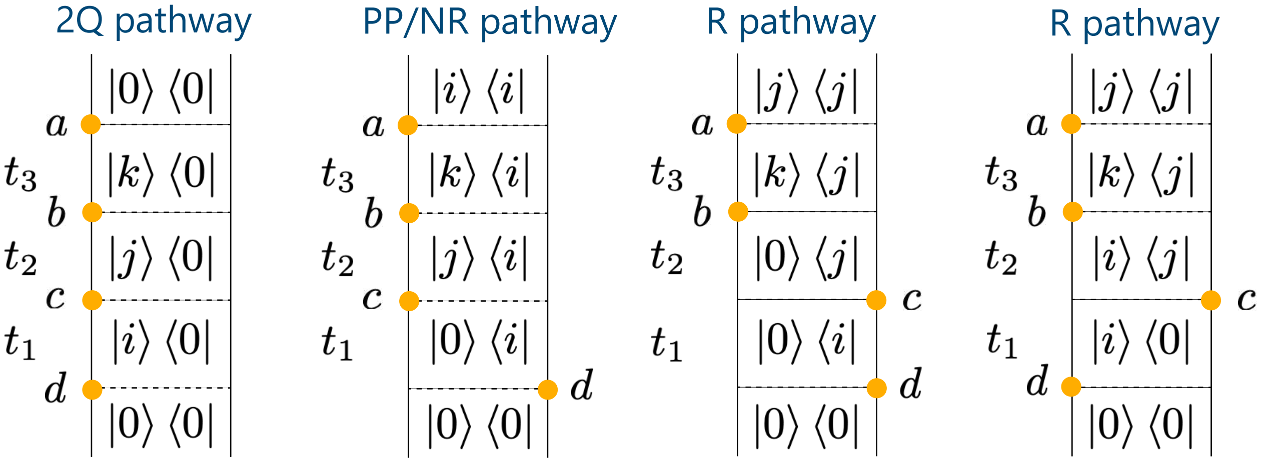

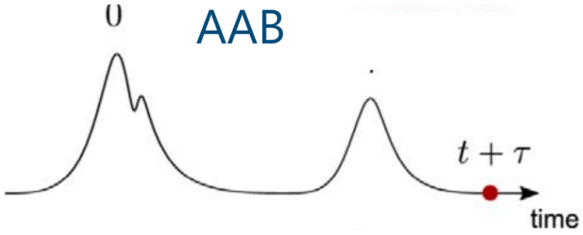

$t_1 = 0,\ t_2 = \tau,\ t_3 = t$

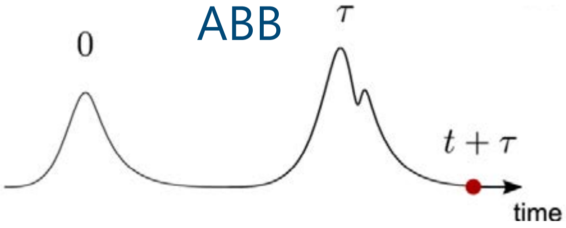

$t_1 = \tau,\ t_2 = 0,\ t_3 = t$

3rd order peaks in 2D THz spectrum of AF mode

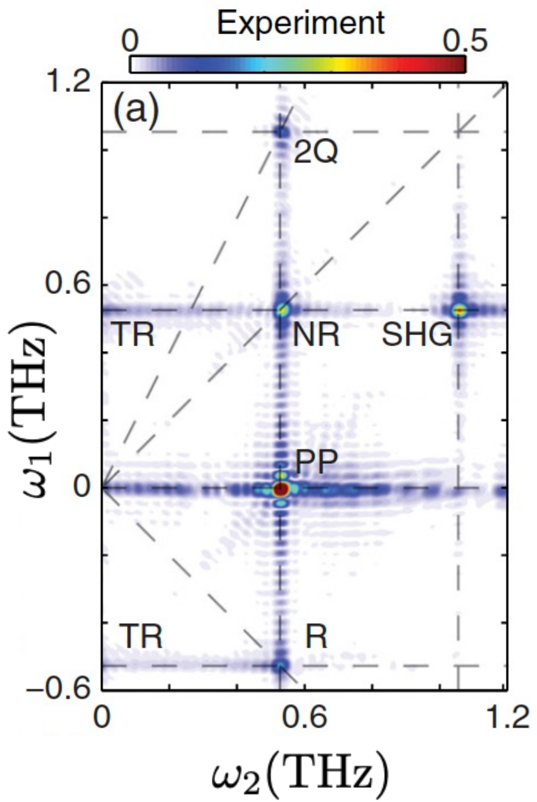

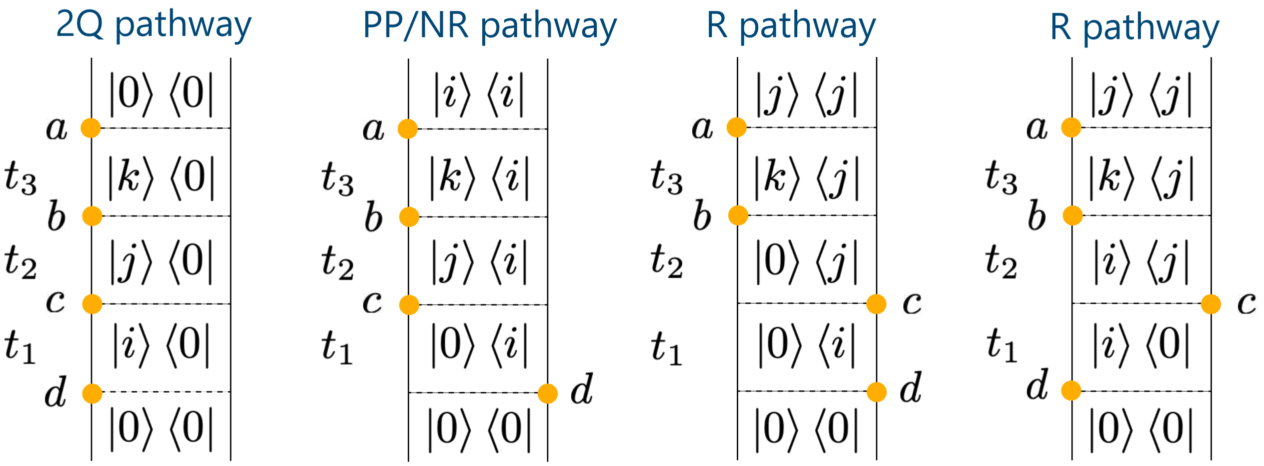

- All third-order signals detected
- 2Q signal can reveal correlations of zone center magnons
- Rephasing (R) signal yields intrinsic broadening

3^{rd} order peaks in 2D THz spectrum of AF mode

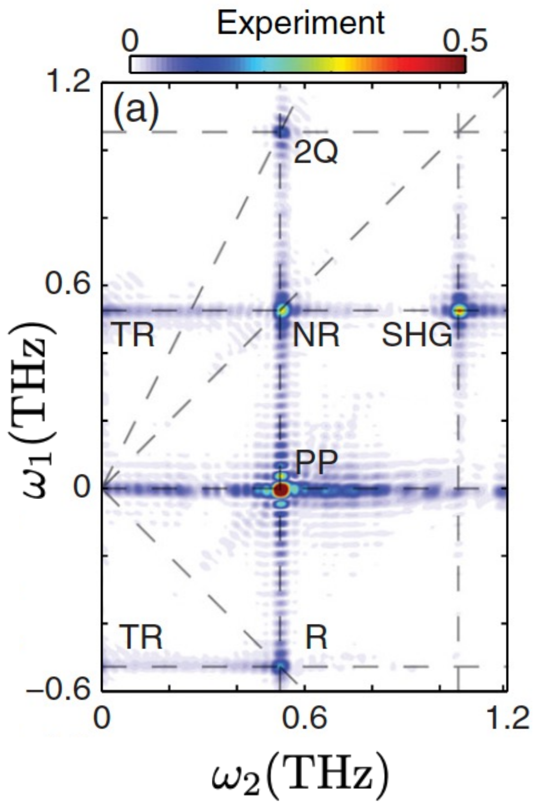

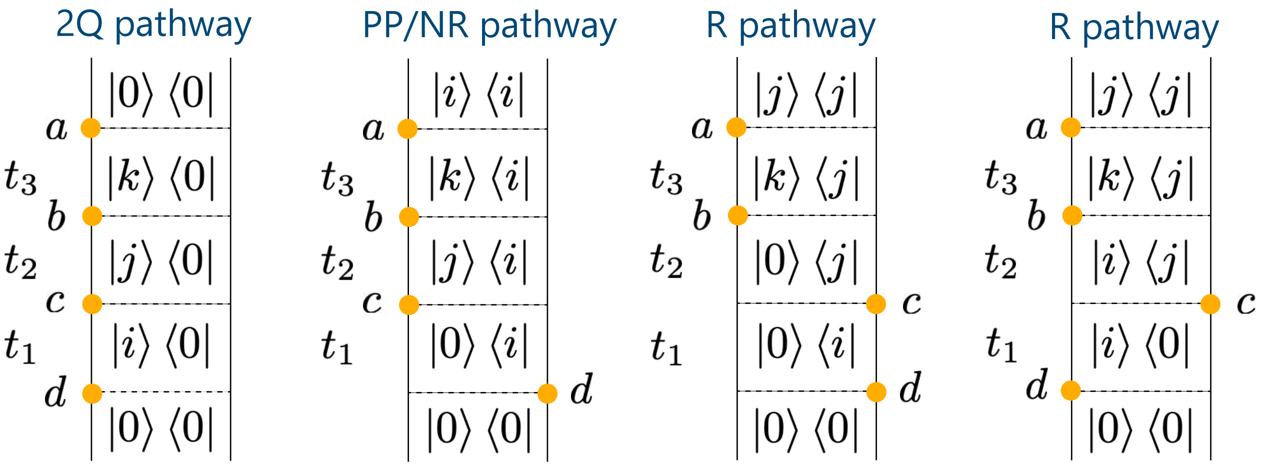

- Future directions
  - Look for mode-mode couplings (off-diagonal peaks)
  - Look for anharmonic magnetic potentials (shifts of diagonal peaks)

Other recent THz 2DCS experiments

UNIVERSITÄT DES SAARLANDES

nature physics

ARTICLES

https://doi.org/10.1038/s41567-020-01149-0

Check for updates

Observation of a marginal Fermi glass

Fahad Mahmood[1,2,3], Dipanjan Chaudhuri[1], Sarang Gopalakrishnan[4,5], Rahul Nandkishore[6] and N. P. Armitage[1]

PHYSICAL REVIEW LETTERS **122**, 073901 (2019)

stion

Distinguishing Nonlinear Terahertz Excitation Pathways with Two-Dimensional Spectroscopy

Courtney L. Johnson, Brittany E. Knighton, and Jeremy A. Johnson*

Department of Chemistry and Biochemistry, Brigham Young University, Provo, Utah 84602, USA

- 2DCS allows to measure intrinsic lifetimes

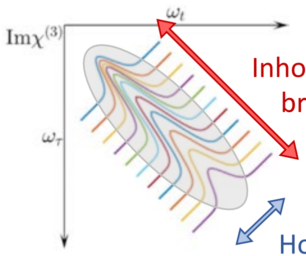

- Distinguish excitation pathways
- Combine THz and Raman pulses

2D spectroscopy of Kitaev honeycomb spin liquid

Kitaev spin model on the honeycomb lattice

$$\hat{H} = -J_x \sum_{\langle ij \rangle_x} \hat{\sigma}_i^x \hat{\sigma}_j^x - J_y \sum_{\langle ij \rangle_y} \hat{\sigma}_i^y \hat{\sigma}_j^y - J_z \sum_{\langle ij \rangle_z} \hat{\sigma}_i^z \hat{\sigma}_j^z$$

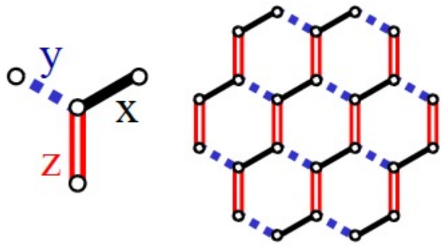

From Yang et al. (2007)

- Exactly solvable in terms of static Z_2 fluxes and Majorana fermions
- Quantum spin liquid ground state with fractionalized excitations
  - How to uniquely identify this state experimentally?

$\sigma_j^a = i b_j^a c_j$ Spins in terms of Majorana fermions

$\hat{u}_{jk} = i b_j^a b_k^a$ Static bond fermions $\{u_{jk} = \pm 1\}$

$\hat{W}_p = \sigma_1^x \sigma_2^y \sigma_3^z \sigma_4^x \sigma_5^y \sigma_6^z$ Z_2 fluxes are conserved

$$\tilde{H} = \sum_{\alpha\,\mathrm{bond}} i \hat{u}_{jk}^{\alpha} c_j c_k$$

$$\Rightarrow \tilde{H}_u = \sum_p \varepsilon_p \left(a_p^\dagger a_p - \frac{1}{2} \right)$$

Kitaev spin model on the honeycomb lattice

$$\hat{H} = -J_x \sum_{\langle ij \rangle_x} \hat{\sigma}_i^x \hat{\sigma}_j^x - J_y \sum_{\langle ij \rangle_y} \hat{\sigma}_i^y \hat{\sigma}_j^y - J_z \sum_{\langle ij \rangle_z} \hat{\sigma}_i^z \hat{\sigma}_j^z$$

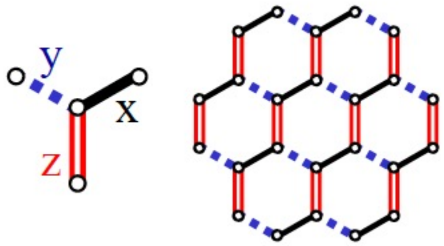

From Yang et al. (2007)

- Exactly solvable in terms of static Z_2 fluxes and Majorana fermions
- Quantum spin liquid ground state with fractionalized excitations
  - How to uniquely identify this state experimentally

From Knolle thesis (2016)

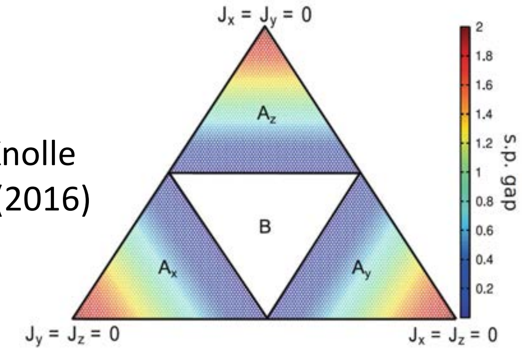

Phase diagram and matter fermion gap

- B phase = gapless spin liquid.
  - Spin correlations only on n.n. bonds
  - Z2 flux gap nonzero
  - Gapless Majorana matter excitations
- A phases = gapped spin liquid
  - Gapped Majorana matter excitations

Linear response: dynamic structure factor

UNIVERSITÄT DES SAARLANDES

- Zero temperature spin correlation function $S_{ij}^{\alpha\beta}(t) = \langle 0|\hat{\sigma}_i^{\alpha}(t)\hat{\sigma}_j^{\beta}(0)|0\rangle,$
- Application of spin σ_i^{α} creates flux pair across bond α and Majorana fermion c at site i $S_{ij}^{\alpha\beta}(\omega) = -i\sum_{\lambda}\langle M_0^{\mathrm{p}}|\hat{c}_i|\lambda\rangle\langle\lambda|\hat{c}_j|M_0^{\mathrm{p}}\rangle\ \delta[\omega-(E_\lambda - E_0^{\mathrm{p}})]\delta_{\langle ij\rangle_\alpha}\delta_{\alpha\beta}.$
- Evaluate dynamic structure factor in the Lehmann representation
- Sites i, j must be nearest-neighbors to allow for flux removal

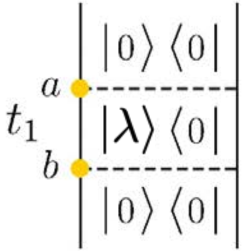

- Intermediate state contains additional flux pair
- States $|\lambda\rangle$ are eigenstates of Hamiltonian with sign of bond variable u_{ij}^{α} flipped

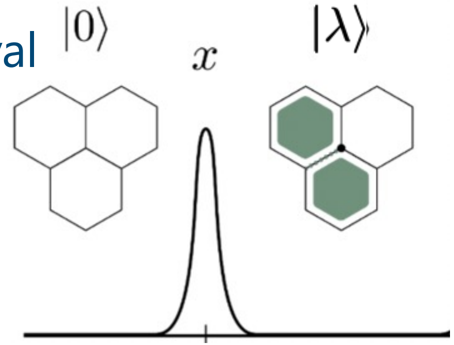

Dynamic structure factor at $q = 0$

- Dynamic structure factor shows broad peak at low energies
- Vanishes below the two-flux gap energy
- Dip at van Hove singularity in the density of states

Isotropic model

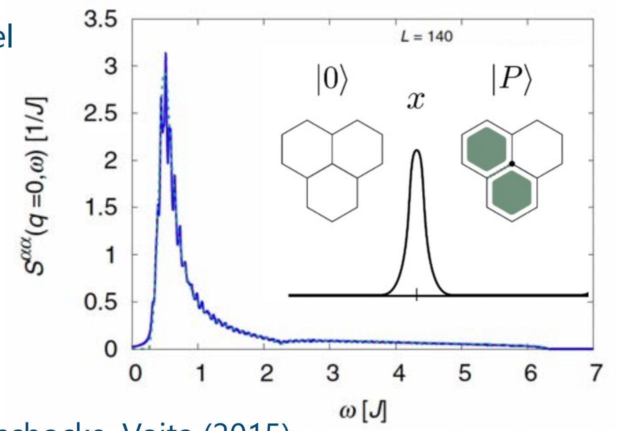

From Zschocke, Vojta (2015)

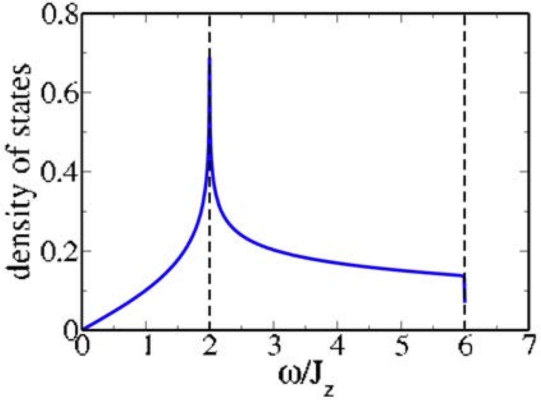

From Knolle *et al.*, PRL (2014)

Nonlinear response at $q = 0$

- 3^{rd} order χ^{zzz} studied by Choi, Lee, Y.-B. Kim (PRL, 2020)
  - Contains fingerprints of fractionalization
  - Vertical signals at two and four-flux gaps
  - Diagonal signal range equals matter bandwidth, axes intercepts yield 4-flux gap

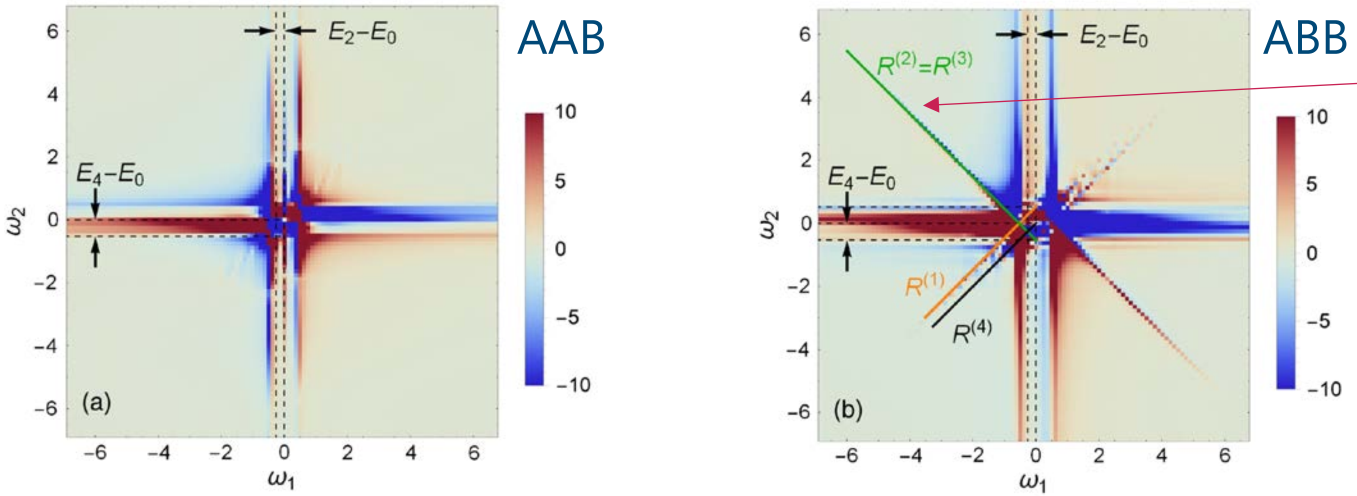

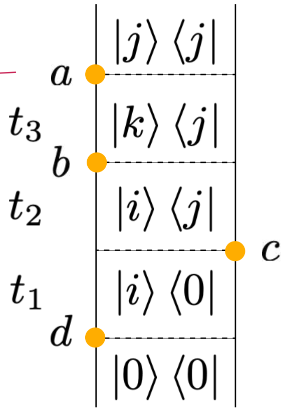

Nonlinear response at $q = 0$

- 3^{rd} order χ^{zzz} studied by Choi, Lee, Y.-B. Kim (PRL, 2020)
  - Contains fingerprints of fractionalization
  - Vertical signals at two and four-flux gaps
  - Diagonal signal range equals matter bandwidth, axes intercepts yield 4-flux gap

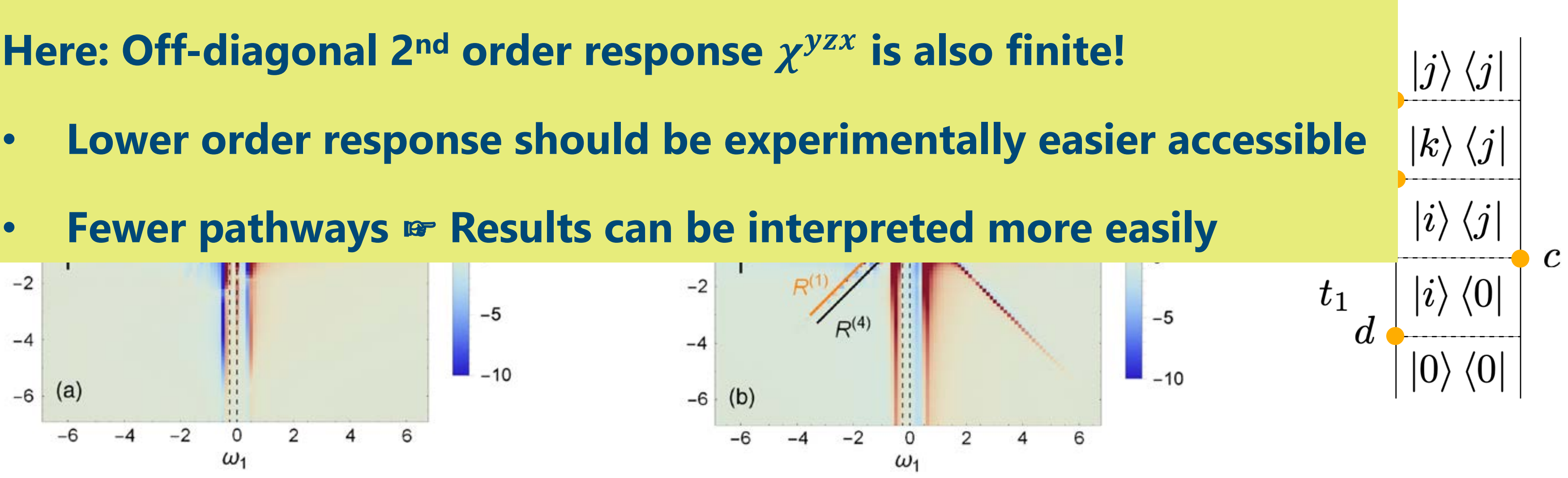

Here: Off-diagonal 2^{nd} order response χ^{yzx} is also finite!

- **Lower order response should be experimentally easier accessible**
- **Fewer pathways ☞ Results can be interpreted more easily**

Second-order 2DCS response at $q = 0$

- 2^{nd} order response for component: (a,b,c) = (y, z, x)

$$\chi^{a,b,c}(\tau_1, \tau_2) = \frac{i^2}{N}\theta(\tau_1)\theta(\tau_2)\langle[[M^a(\tau_1+\tau_2), M^b(\tau_1)], M^c(0)]\rangle$$

$$M^a(t) = \sum_l \sigma_l^a(t)$$

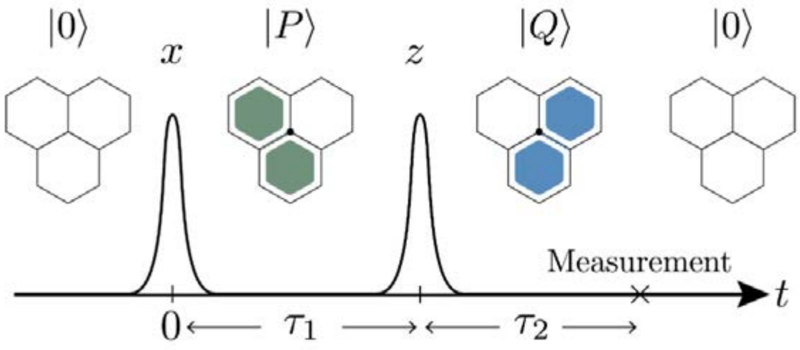

Two pathways

$R^{(1)}$ $R^{(2)}$

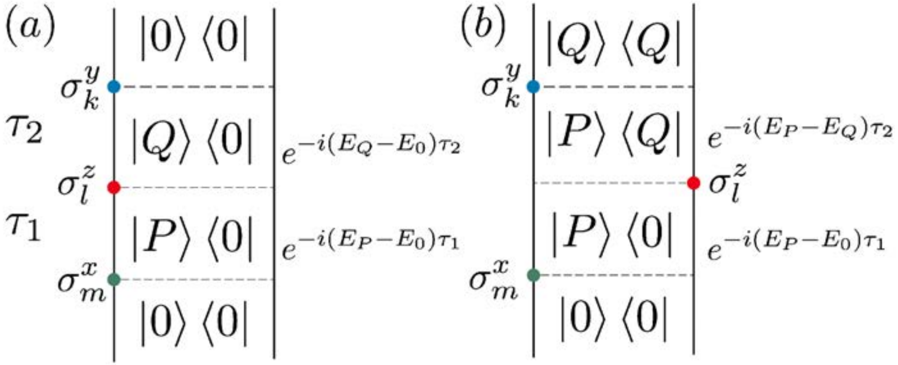

Expressions for the two pathways: R_1 and R_2

$$\chi^{y,z,x}_{R_1}(\tau_1,\tau_2) = -\frac{2}{N}\Re\sum_{PQ}\sum_{klm} \langle 0|\sigma^y_k|Q\rangle\langle Q|\sigma^z_l|P\rangle\langle P|\sigma^x_m|0\rangle \times \theta(\tau_1)\theta(\tau_2)e^{-i\tau_1(E_P-E_0)}e^{-i\tau_2(E_Q-E_0)},$$

$$\chi^{y,z,x}_{R_2}(\tau_1,\tau_2) = +\frac{2}{N}\Re\sum_{PQ}\sum_{klm} \langle 0|\sigma^z_l|Q\rangle\langle Q|\sigma^y_k|P\rangle\langle P|\sigma^x_m|0\rangle \times \theta(\tau_1)\theta(\tau_2)e^{-i\tau_1(E_P-E_0)}e^{-i\tau_2(E_P-E_Q)},$$

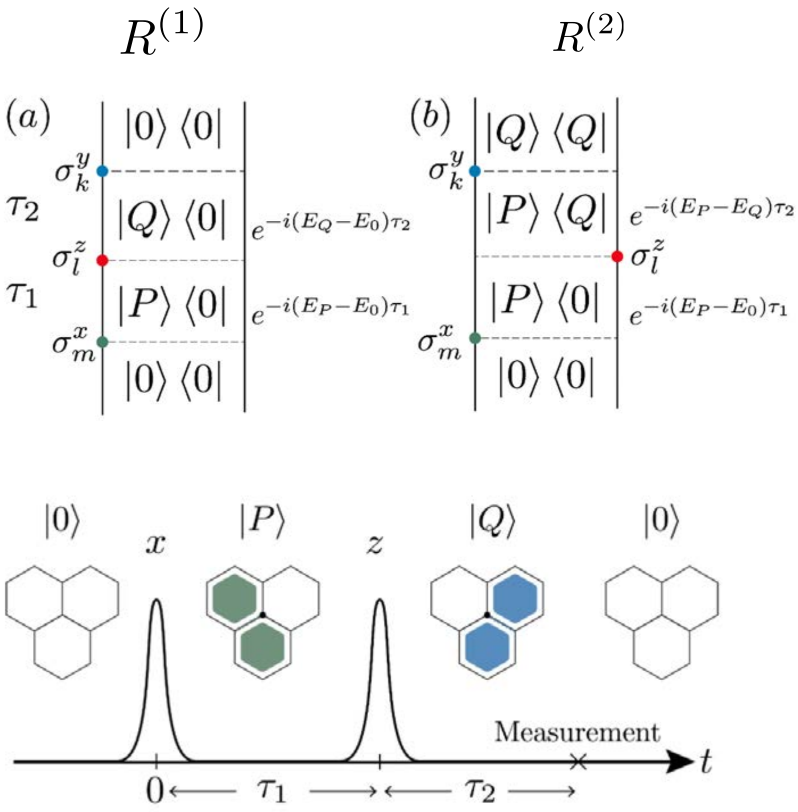

Full second-order 2D spectrum

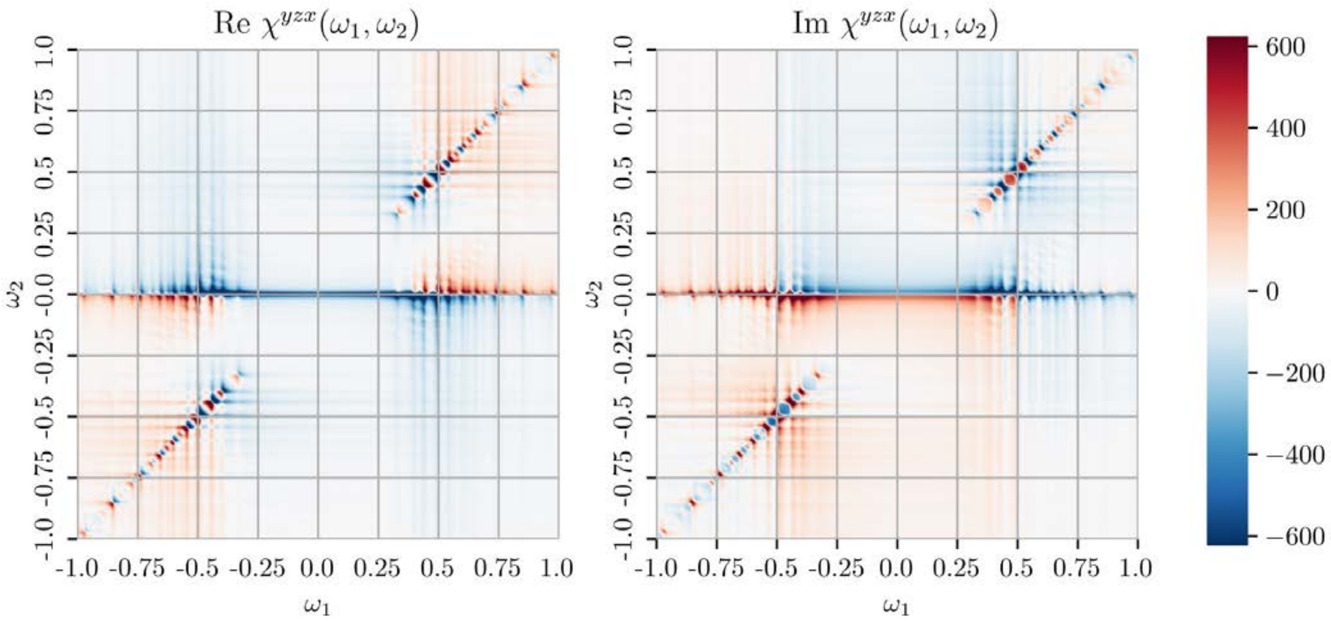

- Time-reversal symmetry requires $\mathrm{Re}\chi^{abc}(\omega_1, \omega_2) = \mathrm{Re}\chi^{abc}(-\omega_1, -\omega_2)$
- Pathways clearly separated $\mathrm{Im}\chi^{abc}(\omega_1, \omega_2) = -\mathrm{Im}\chi^{abc}(-\omega_1, -\omega_2)$

Dominant response at lower energies

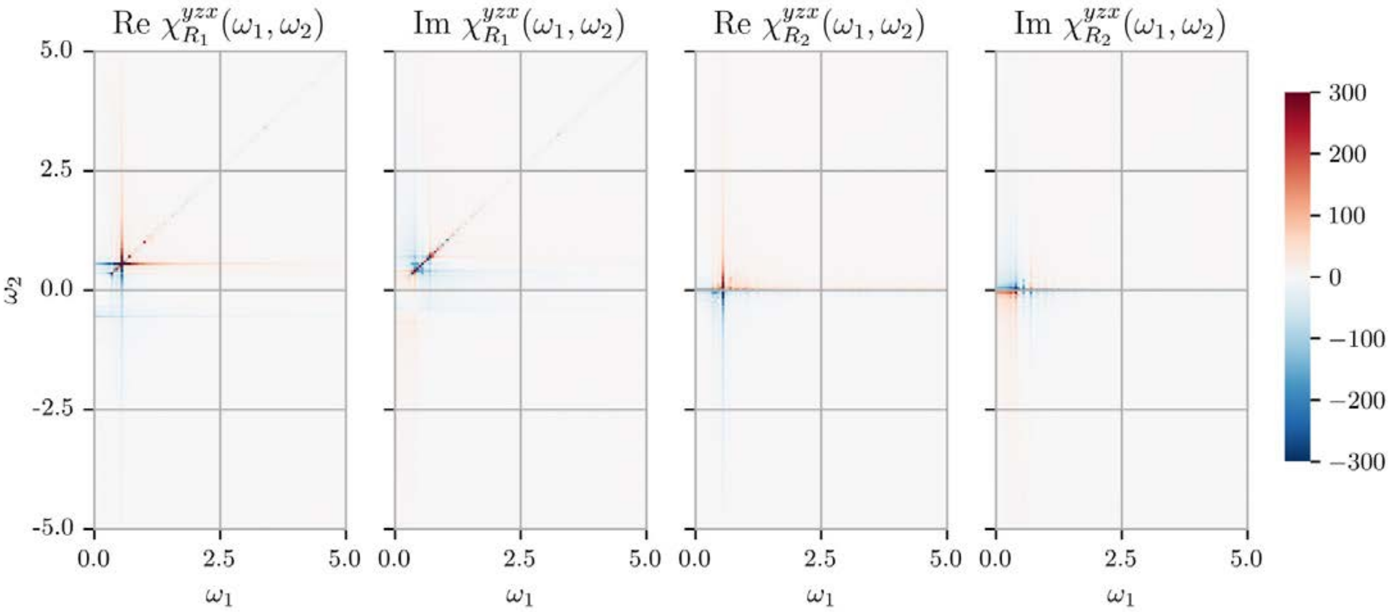

- Real and imaginary parts contain the same information
- Response largest in region $0 < \omega < J$

Interpretation of R_1 pathway

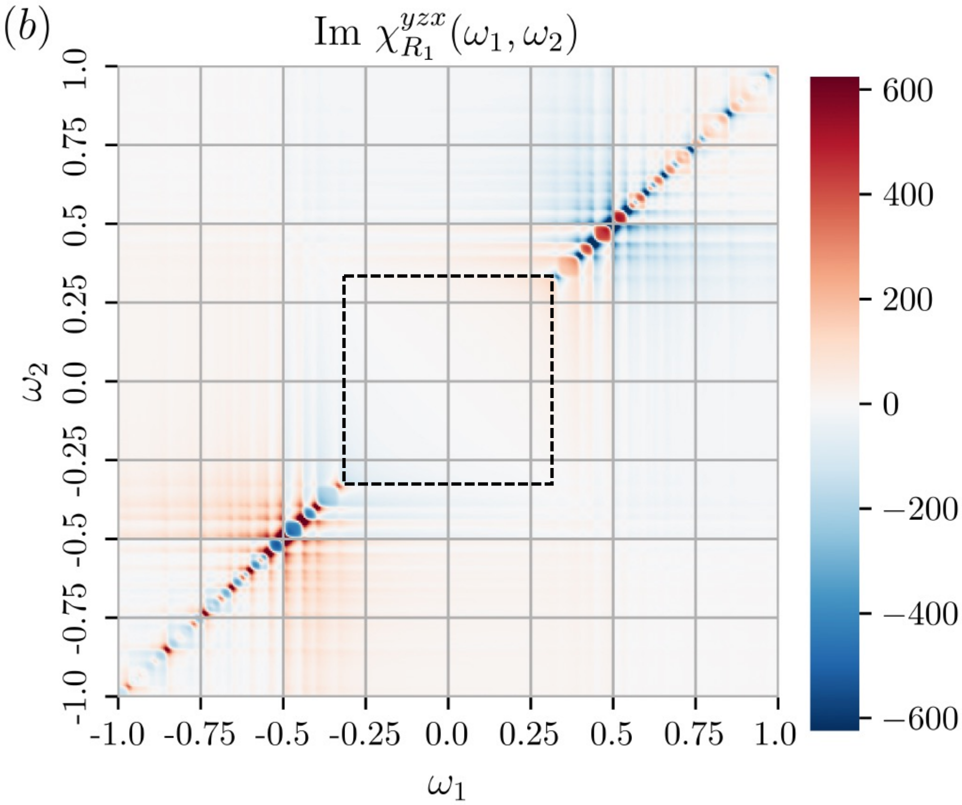

- 2-Flux gap visible
- Continuum of Majorana matter excitations similarly to linear response
- Off-diagonal peaks occur

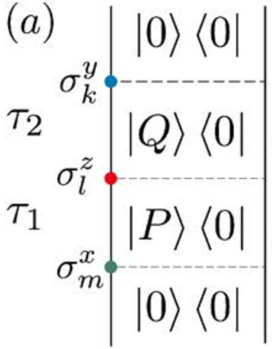

Interpretation of R_2 pathway

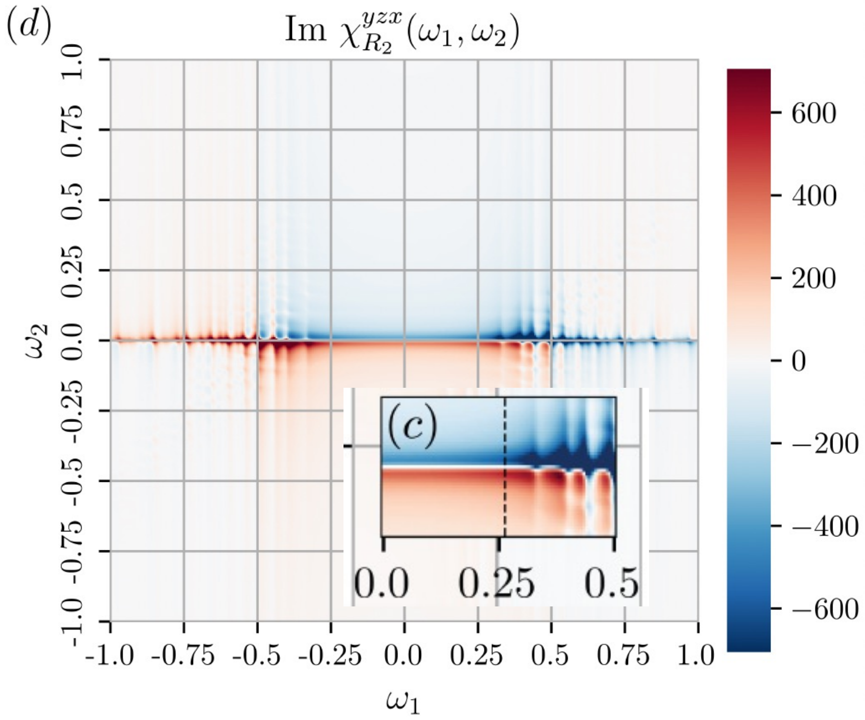

- 2-Flux gap visible as well
- Can distinguish smooth PV from delta-function peaks
- Peaks in ω_2 at energy differences

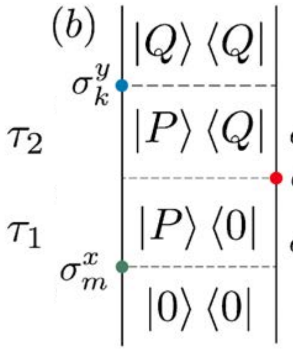

Off-diagonal peaks in R_1

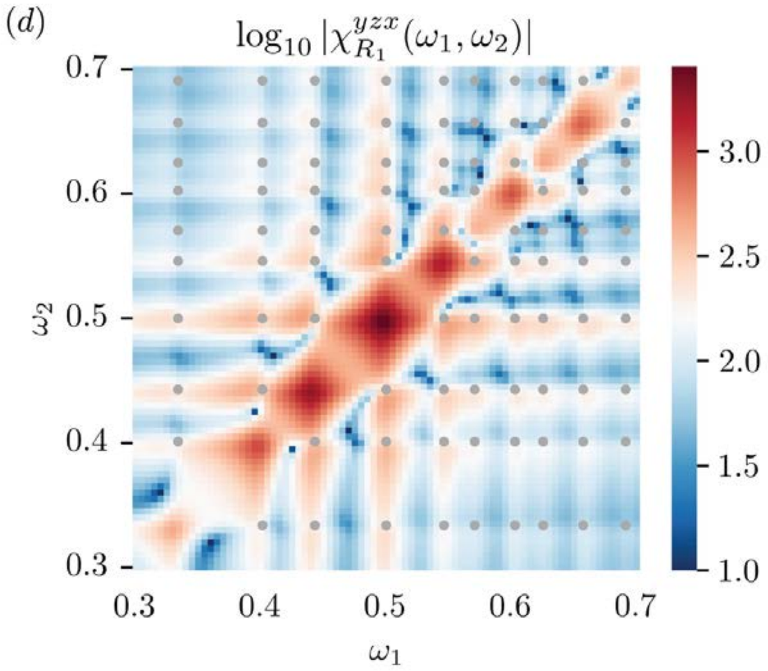

- Grey dots are energies of high IPR wavefunctions $\mathrm{IPR} = \frac{\sum_i |\psi_i|^4}{\sum_i |\psi_i|^2}$
- Response dominated by high IPR states
- Off-diagonal peaks = overlap of localized matter states trapped around Z_2 fluxes

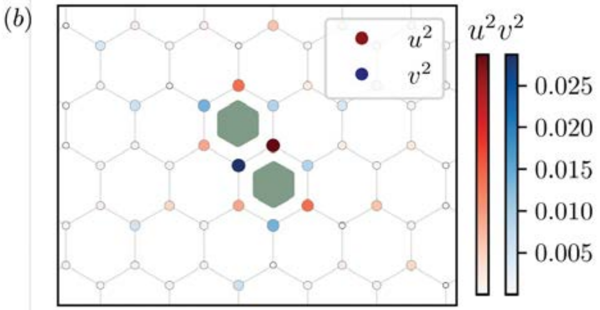

Nonlinear response measures wavefunction properties

Conclusions & Outlook

UNIVERSITÄT DES SAARLANDES

- Nonlinear responses are powerful probes of quantum materials
  - Detect symmetries, reveal hidden orders, symmetry breaking
  - Map out quantum geometry: Berry curvature and quantum metric
  - Access properties of quasiparticles such as lifetimes, couplings & wavefunction overlaps
  - Direct probe of fractionalization in quantum magnets
- Open questions and theory challenges
  - Nonlinear response in correlated and disordered materials
  - 2D spectroscopy of multiferroic and superconducting systems
  - Explore theory of combined nonlinear THz and Raman spectroscopy

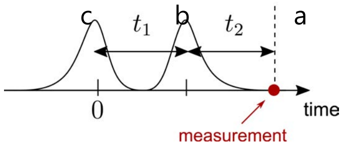

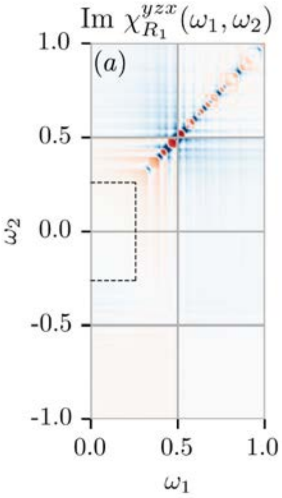

Thank you for your attention!

References

- Sirica, PPO *et al.*, Nat. Mater. (2022).
- Qiang, Quito, Trevisan, PPO, arXiv:2301.11243.